

Sulfur dopant effects on hybrid rGO/MoS₂/PANI nanocomposites for SupercapBattery devices

Murat Ates^{*,1,2}

¹Department of Chemistry/Faculty of Arts and Sciences, Tekirdag Namik Kemal University, TURKIYE

²Nanochem Polymer Energy Company/Silahataraga Mh. University 1st street, Number:13/1 Z102, Tekirdag, TURKIYE

^{*}(mates@nku.edu.tr) Email of the corresponding author

Abstract – In this study, 3 different materials were combined to form hybrid nanocomposite for SupercapBattery applications. The effects of using sulfur (S) doped and undoped reduced graphene oxide (S-rGO), Molybdenum (IV) sulfide (MoS₂), and polyaniline (PANI) were used as a component of nanocomposites. Electrochemical performances were performed by cyclic voltammetry (CV), galvanostatic charge / discharge (GCD) and electrochemical impedance spectroscopy (EIS) measurements. EIS measurements were analyzed by Nyquist, Bode-magnitude, Bode-phase, and Admittance plots. Long-term stability tests were obtained by CV method using 1000 charge/discharge performances at a scan rate of 100 mV×s⁻¹. The highest specific capacitance was calculated as C_{sp}= 1753.77 F×g⁻¹ at 2 mV×s⁻¹ for rGO/MoS₂/PANI nanocomposite.

Keywords – Sulfur Dopant, Hybrid Nanocomposite, S-rGO/MoS₂/PANI, Long Term Stability Test, Double Layer Capacitance

I. INTRODUCTION

The energy storage mechanism divides SCs into two types [1]. These are given as: electrochemical double-layer capacitors (EDLCs) and pseudocapacitors. In EDLCs, the energy is stored electro-statically at the electrode-electrolyte interface in the double layer, while in pseudocapacitors, charge storage occurs via fast redox reactions on the electrode surface.

To improve the energy density of SCs, one design is hybrid supercapacitors (HSCs) that consider the fundamental principles of combining the advantages of batteries and supercapacitors to increase both energy density and power density of HSC devices [2]. In this study, S-doped effect on rGO/MoS₂/PANI hybrid nanocomposite was studied as prepared hybrid nanocomposite with 2032 coin cell in ionic liquid electrolyte.

II. MATERIALS AND METHOD

Electrochemical measurements were performed with 2032 coin-type cells. The slurry was obtained by mixing the as-synthesized

materials, acetylene black and N-methyl-2-pyrrolidone (NMP) as a solvent for materials. Polyvinyl pyrrolidone (PVP) was performed by binder. Then the slurry was pasted onto Al and Cu foils and dried at 60 °C in a vacuum oven for 12 h. The electrolyte was ionic liquid (IL). And the mass loading of electrode of 41.4 mg for rGO/MoS₂/PANI nanocomposite and 14.7 mg for S-rGO/MoS₂/PANI nanocomposite. Galvanostatic charge/discharge, rate performance and cyclic performances were tested between 0.0 and 0.8 V by using ivium-vertex potentiostat-galvanostat instrument.

A. GO and rGO synthesis

Graphene oxide (GO) was synthesized from graphite powder according to modified Hummers method [3]. GO was reduced by microwave-irradiation method at 180 W and 10 min. [4, 5].

B- S-rGO synthesis

In literature, the conductivity of GO increases by doped of S and N elements [6, 7]. As

a result, S doped GO have a superior performance compared to other additives (N, B or P) in terms of capacitor performance [8]. 5 ml Na_2S was mixed in various sources (0.5 M). It was synthesized in a microwave oven at 180 Watt and 20 min. So, S-GO was obtained by centrifuged 3 times [9].

C- MoS_2 synthesis

0.6653 g sodium molybdate (VI) dihydrate ($\text{NaMoO}_4 \times 2\text{H}_2\text{O}$) and 0.8453 g of thiourea (H_2NCSNH_2) were dissolved in 33 ml of deionized (DI) water. The mixture was then transferred to a hydrothermal synthesis reactor (autoclave) for 24 h at 210 °C. After annealing, the solution was removed and the resulting precipitates were immersed in DI water and sonicated for 30 min. Excess impurities were removed from the mixture by centrifugation 5 times at 4000 rpm for 15 min. Thus, MoS_2 nanomaterial was synthesized [10].

D- Polyaniline (PANI) synthesis

Aniline (0.2 ml) and sodium dodecyl benzene sulphate (SDBS, 3.3 g) as a surfactant will be mixed with 0.06 ml of H_3PO_4 in 10 ml of DI water in an ice-bath. The resulting ANI/ H_3PO_4 salt will be added to the 0.46 g / 5 ml DI water soluble ammonium persulfate (APS) mixture. Polymerization will continue in the ice-bath for 12 h. A green colour solid PANI will be formed. The resulting solid PANI will be dried by DI water and ethyl alcohol [11].

III. RESULTS & DISCUSSION

E- Electrochemical performances of SupercapBattery device

Electrochemical performances of rGO/ MoS_2 /PANI and S-rGO/ MoS_2 /PANI nanocomposites were performed by CV, GCD and EIS measurements.

F- CV measurements

CV plots of rGO/ MoS_2 /PANI and S-rGO/ MoS_2 /PANI nanocomposites at different scan rates from 1000 $\text{mV} \times \text{s}^{-1}$ to 100 $\text{mV} \times \text{s}^{-1}$ were given in Figure 1.

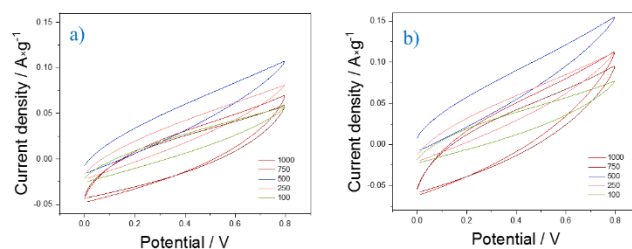


Fig. 1 CV plots of a) rGO/ MoS_2 /PANI, b) S-rGO/ MoS_2 /PANI nanocomposites at different scan rates from 1000 to 100 $\text{mV} \times \text{s}^{-1}$.

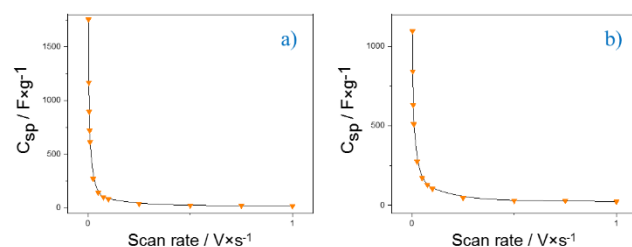


Fig. 2 C_{sp} vs. Scan rate plot of a) rGO/ MoS_2 /PANI, b) S-rGO/ MoS_2 /PANI nanocomposites at different scan rates from 1000 to 2 $\text{mV} \times \text{s}^{-1}$.

The highest specific capacitances were presented as $C_{sp} = 1753.77 \text{ F} \times \text{g}^{-1}$ and $C_{sp} = 1094.81 \text{ F} \times \text{g}^{-1}$ at a scan rate of 2 $\text{mV} \times \text{s}^{-1}$ for rGO/ MoS_2 /PANI and S-rGO/ MoS_2 /PANI nanocomposites, respectively. The lowest specific capacitances were obtained for highest scan rates (1000 $\text{mV} \times \text{s}^{-1}$). The specific capacitances were taken as $C_{sp} = 17.24 \text{ F} \times \text{g}^{-1}$ and $C_{sp} = 22.65 \text{ F} \times \text{g}^{-1}$ at a scan rate of 1000 $\text{mV} \times \text{s}^{-1}$ for rGO/ MoS_2 /PANI and S-rGO/ MoS_2 /PANI nanocomposites, respectively.

G- GCD measurements

GCD plots of rGO/ MoS_2 /PANI and S-rGO/ MoS_2 /PANI nanocomposites were given at constant current density from 0.1 $\text{A} \times \text{g}^{-1}$ to 1.0 $\text{A} \times \text{g}^{-1}$ as shown in Figure 3. The highest specific capacitance was obtained as $C_{sp} = 1.54 \text{ F} \times \text{g}^{-1}$ at 0.1 mA for rGO/ MoS_2 /PANI nanocomposite by GCD measurements. In addition, it was obtained as $C_{sp} = 2.02 \text{ F} \times \text{g}^{-1}$ at 0.1 mA for S-rGO/ MoS_2 /PANI nanocomposites by GCD method.

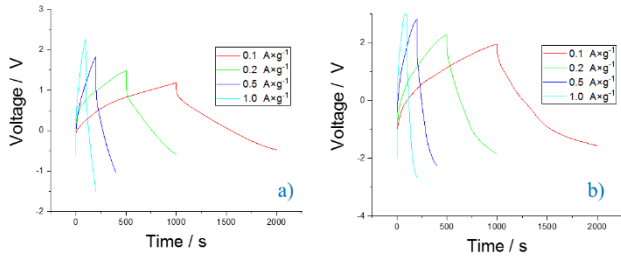


Fig. 3 GCD plots of a) rGO/MoS₂/PANI, b) S-rGO/MoS₂/PANI nanocomposites at constant current density from 0.1 A×g⁻¹ to 1.0 A×g⁻¹.

H-EIS measurements

EIS plots of rGO/MoS₂/PANI and S-rGO/MoS₂/PANI nanocomposites were given in Figure 4. Specific capacitance was obtained as $C_{sp} = 0.325 \text{ F} \times \text{g}^{-1}$ for S-rGO/MoS₂/PANI nanocomposite obtained from Nyquist plot (Fig.4).

Double layer capacitance (C_{dl}) and phase angle (θ) were obtained as $C_{dl} = 0.29 \text{ F} \times \text{g}^{-1}$ and $\theta = 27.05^\circ$ at 0.015 Hz for rGO/MoS₂/PANI nanocomposite obtained from Bode-magnitude and Bode-phase plots, respectively. The other C_{dl} and θ values were obtained as $C_{dl} = 0.21 \text{ F} \times \text{g}^{-1}$ and $\theta = 49.97^\circ$ at 0.0019 Hz for S-rGO/MoS₂/PANI nanocomposite, respectively (Fig.5). Admittance plots defined conductivity of nanocomposite materials as $Y'' = 0.0017 \text{ S}$ for rGO/MoS₂/PANI, and $Y'' = 0.000425 \text{ S}$ for S-rGO/MoS₂/PANI nanocomposites as shown in Figure 5.

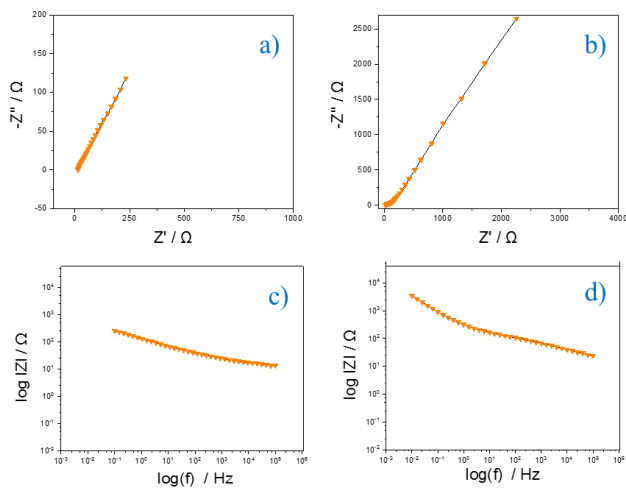


Fig. 4 EIS plots of Nyquist plots a) rGO/MoS₂/PANI, b) S-rGO/MoS₂/PANI nanocomposites, Bode-magnitude plots c) rGO/MoS₂/PANI, d) S-rGO/MoS₂/PANI nanocomposites.

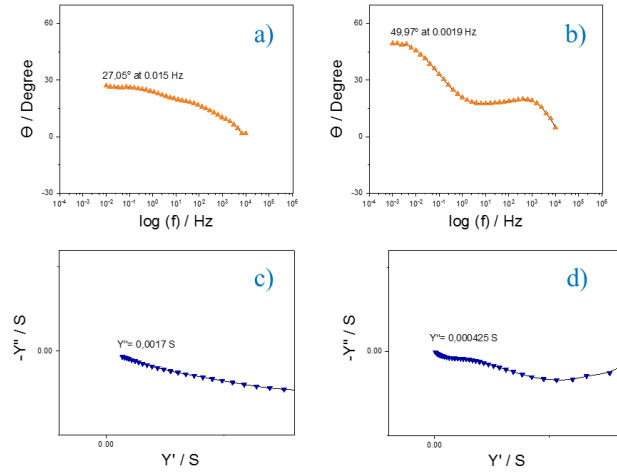


Fig. 5 EIS plots of Bode-phase plots a) rGO/MoS₂/PANI, b) S-rGO/MoS₂/PANI nanocomposites, Admittance plots a) rGO/MoS₂/PANI, b) S-rGO/MoS₂/PANI nanocomposites.

J- Stability tests

The stability graphs of the rGO/MoS₂/PANI and S-rGO/MoS₂/PANI nanocomposites for 2032 coin cell electrodes were given charge/discharge device performances for 1000 cycles (Fig.6). The first capacitance value after 1000 charge/discharge performances were obtained as 92.38% for rGO/MoS₂/PANI nanocomposite, and 88.74% for S-rGO/MoS₂/PANI nanocomposites in ionic liquid in 2032 coin cell.

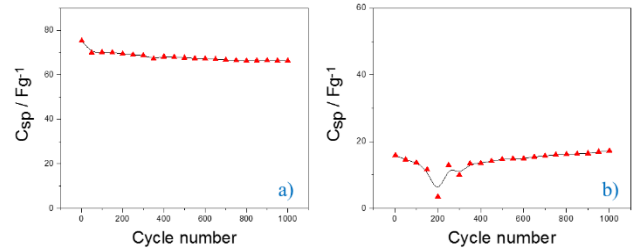


Fig. 6 Stability tests of a) rGO/MoS₂/PANI, b) S-rGO/MoS₂/PANI nanocomposites. The measurements were taken at a scan rate of 100 mV×s⁻¹, 1000 charge-discharge measurements.

IV. CONCLUSION

SupercapBattery device performances were obtained by 2032 coin cell. The highest energy and power densities were obtained as $E = 1.95 \text{ Wh} \times \text{kg}^{-1}$ at 0.1 mA and $E = 5.37 \text{ Wh} \times \text{kg}^{-1}$ at 5 mA and $P = 714.98 \text{ W} \times \text{kg}^{-1}$ at 10 mA and $P = 1725 \text{ W} \times \text{kg}^{-1}$ at 10 mA for rGO/MoS₂/PANI and S-rGO/MoS₂/PANI nanocomposites, respectively.

Phase angles were also presented as $\theta = 27.05^\circ$ at 0.015 Hz for rGO/MoS₂/PANI

nanocomposite and $\theta = 49.97^\circ$ at 0.0019 Hz for S-rGO/MoS₂/PANI nanocomposite from EIS data. The highest initial capacitance preservation was obtained as 92.38% for rGO/MoS₂/PANI nanocomposite and 88.74% for S-rGO/MoS₂/PANI nanocomposites for 1000 charge-discharge measurements.

Our results have demonstrated that rGO/MoS₂/PANI and S-rGO/MoS₂/PANI nanocomposites for 2032 coin cell electrodes will be considered as a promising symmetrical electrode materials for the next generation of supercapacitor applications.

ACKNOWLEDGMENT

Authors thank to TUBITAK, Teydeb-1512 project for material and device support.

REFERENCES

- [1] MM Vadiyar, SC Bhise, SK Patil, SS Kolekar, JY Chang, AV Ghule, "Comparative study of individual and mixed aqueous electrolytes with ZnFe₂O₄ nanoflakes thin film as an electrode for supercapacitor application", *ChemistrySelect*, vol. 1, pp. 059-966, 2016.
- [2] R. Ahmad, N. Iqbal, MM Baig, T Noor, G Ali, IH Gul, "ZIF-67 derived nitrogen doped CNTs decorated with sulfur and Ni(OH)₂ as potential electrode material for high-performance supercapacitor", *Electrochim. Acta*, vol. 364, Article number: 137147, 2020.
- [3] Z. Zhang, Z. Wei, M. Won, "Nanostructures of Polyaniline doped with inorganic acids", *Macromolecules*, vol. 35, pp. 5937-5942, 2002.
- [4] M Ates, O Yoruk, Y Bayrak, "Binary nanocomposites of reduced graphene oxide and cobalt (II, III) oxide for supercapacitor devices", *Materials Technology: Advanced Performance Materials*, vol. 37(9), pp. 1168-1182, 2022.
- [5] O Yoruk, Y Bayrak, M Ates, "Design and assembly of supercapacitor based on reduced graphene oxide / TiO₂ / Polyaniline ternary nanocomposite and its application in electrical circuit", *Polymer Bulletin*, vol. 79, pp. 2969-2993, 2022.
- [6] XL Ma, GQ Ning, YF Kan, YM Ma, CL Qi, B Chen, YF Li, XY Lan, JS Gao, "Synthesis of S-doped mesoporous carbon fibres with ultra-high S concentration and their application as high performance electrodes in supercapacitors", *Electrochim. Acta*, vol. 150, pp. 108-113, 2014.
- [7] XT Sun, WT Shi, L Xiang, WC Zhu, "Controllable synthesis of magnesium oxysulfate, Nanowires with different morphologies", *Nanoscale Res. Lett.*, vol. 3, pp. 386-389, 2008.
- [8] WJ Si, J Zhou, SM Zhang, SJ Li, W Xing, SP Zhua, "Tunable N-doped or dual N, S-doped activated hydrothermal carbons derived from human hair and glucose for supercapacitor applications", *Electrochim. Acta*, vol. 107, pp. 397-405, 2013.
- [9] NHA Rosli, KS Lau, T Winie, SX Chin, CH Chia, "Synergistic effect of sulfur-doped reduced graphene oxide created via microwave-assisted synthesis for supercapacitor applications", *Diamond & Related Materials*, vol. 120, Article number: 108696, 2021.
- [10] Ramachandran T., Dhayabaran V.V. 2019. "Utilization of a MnO₂/polythiophene/rGO nanocomposite modified glassy carbon electrode as an electrochemical sensor for methyl parathion", Received, Springer Science+Business Media, LLC, part of Springer Nature 2019.
- [11] M. Ates, O. Kuzgun, "Modified carbon black, CB/MnO₂ and CB/MnO₂/PPy nanocomposites synthesized by microwave-assisted method for energy storage devices with high electrochemical performances", *Plastics Rubber and Composites*, vol. 49(8), pp. 342-356, 2020.